Kubo formula for Floquet states and photoconductivity oscillations in a two-dimensional electron gas

Manuel Torres[1,*] and Alejandro Kunold[2,†]
[1]*Instituto de Física, Universidad Nacional Autónoma de México, Apartado Postal 20-364, México Distrito Federal, 01000, Mexico*
[2]*Departamento de Ciencias Básicas, Universidad Autónoma Metropolitana-Azcapotzalco, Avenida San Pablo 180, México Distrito Federal, 02200, Mexico*
(Received 24 August 2004; revised manuscript received 23 November 2004; published 21 March 2005)

The recent discovery of the microwave-induced vanishing resistance states in a two-dimensional electron system (2DES) is an unexpected and surprising phenomenon. In these experiments the magnetoresistance of a high mobility 2DES under the influence of microwave radiation of frequency ω at moderate values of the magnetic field exhibits strong oscillations with zero-resistance states (ZRS) governed by the ratio ω/ω_c, where ω_c is the cyclotron frequency. In this work we present a model for the photoconductivity of a 2DES subjected to a magnetic field. The model includes the microwave and Landau contributions in a nonperturbative, exact way, while impurity-scattering effects are treated perturbatively. In our model, the Landau-Floquet states act coherently with respect to the oscillating field of the impurities that in turn induces transitions between these levels. Based on this formalism, we provide a Kubo-like formula that takes into account the oscillatory Floquet structure of the problem. We study the effects of both short-range and long-range disorder on the photoconductivity. Our calculation yields a magnetoresistance oscillatory behavior with the correct period and phase. It is found that, in agreement with experiment, negative dissipation can only be induced in very high mobility samples. We analyze the dependence of the results on the microwave power and polarization. For high-intensity radiation, multiphoton processes take place predicting negative-resistance states centered at $\omega/\omega_c=\frac{1}{2}$ and $\omega/\omega_c=\frac{3}{2}$.

DOI: 10.1103/PhysRevB.71.115313 PACS number(s): 73.43.−f, 72.40.+w, 75.47.−m

I. INTRODUCTION

Two-dimensional electron systems (2DES) in a perpendicular, strong magnetic field have been extensively studied in relation with the quantum Hall effect. Recently, two experimental groups[1–4] reported the observation of a unique phenomenon: the existence of zero-resistance states (ZRS) in an ultraclean $GaAs/Al_xGa_{1-x}As$ sample subjected to microwave radiation and moderate magnetic fields. The magnetoresistance exhibits strong oscillations with ZRS governed by the ratio $\epsilon=\omega/\omega_c$, where ω_c is the cyclotron frequency. According to Zudov *et al.*,[3] the oscillation amplitudes reach maxima at $\epsilon=\omega/\omega_c=j$ and minima at $\epsilon=j+\frac{1}{2}$, for j, an integer. On the other hand Mani *et al.*[2] reported also a periodic oscillatory behavior, but with maxima at $\epsilon=j-\frac{1}{4}$ and minima at $\omega/\omega_c=j+\frac{1}{4}$. Additionally, experimental work appeared recently.[5–9]

In spite of a large number of theoretical works,[10–20] a complete understanding of the effects in 2DES induced by microwaves has not yet been achieved. A pioneering work put forward by Ryzhii[10] and another by Ryzhii and Suris[11] predicted the existence of negative-resistance states (NRS). Durst *et al.*[12] found also NRS in a a diagrammatic calculation of the photoexcited electron scattered by a disorder potential. A possible connection between the calculated NRS and the observed vanishing resistance was put forward in Ref. 13, noting that a general analysis of Maxwell equations shows that negative resistance induces an instability that drives the system into a ZRS. Whereas some of the models[10–12,17] are based on impurity-assisted mechanisms, there are alternative explanations[5,19,20] in which the leading contribution arises from the modifications of the electron distribution function induced by the microwave radiation. These models, as well as some of their predictions, remain to be tested experimentally.

In this work we present a model which includes the Landau and radiation contribution (in the long-wavelength limit) in a nonperturbative exact way. Impurity scattering effects are treated perturbatively. With respect to the Landau-Floquet states, the impurities act as a coherent oscillating field which induces the transitions that prove to be essential in order to reproduce the observed oscillatory behavior of the magnetoresistance. Based on this formalism a Kubo-like expression for the conductance is provided. Our results display a strong oscillatory behavior for ρ_{xx} with NRS. It is found that ρ_{xx} vanishes at $\epsilon=\omega/\omega_c=j$ for j integer. The oscillations follow a pattern with minima at $\epsilon=j+\delta$ and maxima at $\epsilon=j-\delta$, adjusted with $\delta\approx\frac{1}{5}$. The model is used to test chirality effects induced by the magnetic field, and calculations are carried out for various $\boldsymbol{E}$-field polarizations. Finally, we explore the nonlinear regime in which multiphoton processes play an essential role.

The paper is organized as follows. In the next section we present the model and the method that allows us to obtain the exact solution of the Landau-microwave system as well as the perturbative corrections induced by the impurity potential. In Sec. III we develop the formulation of dc electrical linear response theory valid in arbitrary magnetic fields and microwave radiation. A discussion of relevant numerical calculations is presented in Sec. IV. Section V contains a summary of our main results. Details of the calculations are summarized in the Appendixes.

II. THE MODEL

We consider the motion of an electron in two dimensions subject to a uniform magnetic field **B** perpendicular to the plane and driven by microwave radiation. In the long-wave limit the dynamics is governed by the Schrödinger equation,

$$i\hbar \frac{\partial \Psi}{\partial t} = H\Psi = [H_{\{B,\omega\}} + \tilde{V}(\boldsymbol{r})]\Psi. \tag{1}$$

Here $H_{\{B,\omega\}}$ is the Landau Hamiltonian coupled to the radiation field (with $\lambda \to \infty$) and $\tilde{V}(\boldsymbol{r})$ is any potential that can can be decomposed in a Fourier expansion. The method applies in general if $\tilde{V}(\boldsymbol{r})$ includes various possible effects such as lattice periodic potential, finite wavelength corrections, impurity scattering, etc.; however, as it will be lately argued, the impurity scattering is the most likely explanation for the recent experimental results. One important remark with relation to the impurity potential in Eq. (1) is that to start with, it should only include the polarization effects produced by the combined effects of the Landau-Floquet states and the impurity potentials. The broadening effects produced by this potential are, as usual, included through the Kubo formula. Then we write $\tilde{V}(\boldsymbol{r})$ as

$$\tilde{V}(\boldsymbol{r}) = V(\boldsymbol{r}) - \Delta V(\boldsymbol{r}), \quad \Delta V(\boldsymbol{r}) = W^{\dagger} V(\boldsymbol{r}) W, \tag{2}$$

where W is the transformation that takes exactly into account the microwave-Landau dynamics; it is explicitly given in Eq. (10). In the absence of the microwave radiation, $W \equiv 1$ and $\tilde{V}(\boldsymbol{r})$ vanishes. The impurity scattering potential $V(\boldsymbol{r})$ is decomposed as

$$V(\boldsymbol{r}) = \sum_i \int \frac{d^2 q}{(2\pi)^2} V(\boldsymbol{q}) \exp\{i\boldsymbol{q} \cdot (\boldsymbol{r} - \boldsymbol{r}_i)\}. \tag{3}$$

Here $\boldsymbol{r}_i$ is the position of the i^{th} impurity and the explicit form of $V(\boldsymbol{q})$ depends on the mechanism that applies under particular physical conditions. Some examples will be considered in Sec. IV. $H_{\{B,\omega\}}$ is then written as

$$H_{\{B,\omega\}} = \left(\frac{1}{2m^*}\right)\boldsymbol{\Pi}^2, \quad \boldsymbol{\Pi} = \mathbf{p} + e\mathbf{A}, \tag{4}$$

where m^* is the effective electron mass and the vector potential **A** includes the external magnetic and radiation fields (in the $\lambda \to \infty$ limit) contributions

$$\mathbf{A} = -\left(\frac{1}{2}\right)\boldsymbol{r} \times \boldsymbol{B} + \mathrm{Re}\left[\left(\frac{\boldsymbol{E}_0}{\omega}\right)\exp\{-i\omega t\}\right]. \tag{5}$$

We first consider the exact solution of the microwave-driven Landau problem. The impurity-scattering effects are lately added perturbatively. This approximation is justified on the following conditions: (i) $|V|/\hbar\omega_c \ll 1$ and (ii) $\omega\tau_{tr} \sim \omega_c \tau_{tr} \gg 1$; τ_{tr} is the transport relaxation time that is estimated using its relation to the electron mobility $\mu = e\tau_{tr}/m^*$. As discussed in Sec. IV both conditions are fully complied.

The system posed by $H_{\{B,\omega\}}$ can be recast as a forced harmonic oscillator, a problem that was solved a long time ago by Husimi.[21] Following the formalism developed in Refs. 22,23, we introduce a canonical transformation to new variables Q_μ, P_μ; $\mu = 0, 1, 2$, according to

$$Q_0 = t, \quad P_0 = i\partial_t + e\phi + e\boldsymbol{r} \cdot \boldsymbol{E},$$

$$\sqrt{eB} Q_1 = \Pi_y, \quad \sqrt{eB} P_1 = \Pi_x,$$

$$\sqrt{eB} Q_2 = p_x + eA_x + eBy, \quad \sqrt{eB} P_2 = p_y + eA_y - eBx. \tag{6}$$

It is easily verified that the transformation is indeed canonical; and the new variables obey the commutation rules, $-[Q_0, P_0] = [Q_1, P_1] = [Q_2, P_2] = i$, all other commutators being zero. The inverse transformation gives

$$x = l_B(Q_1 - P_2), \quad y = l_B(Q_2 - P_1), \tag{7}$$

where $l_B = \sqrt{\hbar / eB}$ is the magnetic length. The operators (Q_2, P_2) can be identified with the generators of the electric-magnetic translation symmetries.[24–26] Final results are independent of the selected gauge. From the operators in Eq. (6) we construct two pairs of harmonic oscillatorlike ladder operators, $(a_1, a_1^\dagger)$, and $(a_2, a_2^\dagger)$, with

$$a_1 = \sqrt{\frac{1}{2}}(P_1 - iQ_1), \quad a_2 = \sqrt{\frac{1}{2}}(P_2 - iQ_2), \tag{8}$$

obeying $[a_1, a_1^\dagger] = [a_2, a_2^\dagger] = 1$ and $[a_1, a_2] = [a_1, a_2^\dagger] = 0$.

It is now possible to find a unitary transformation that exactly diagonalizes $H_{\{B,\omega\}}$; it yields

$$W^\dagger H_{\{B,\omega\}} W = \omega_c\left(\tfrac{1}{2} + a_1^\dagger a_1\right) \equiv H_0, \tag{9}$$

with the cyclotron frequency $\omega_c = eB/m^*$ and the $W(t)$ operator given by

$$W(t) = \exp\{i\eta_1 Q_1\}\exp\{i\xi_1 P_1\}\exp\{i\eta_2 Q_2\} \times \exp\{i\xi_2 P_2\}\exp\left\{-i\int^t \mathcal{L} dt'\right\}, \tag{10}$$

where the functions $\eta_i(t)$ and $\xi_i(t)$ represent the solutions to the classical equations of motion that follow from the variation of the Lagrangian:

$$\mathcal{L} = \left(\frac{\omega_c}{2}\right)(\eta_1^2 + \zeta_1^2) + (\dot{\zeta}_1 \eta_1 + \dot{\zeta}_2 \eta_2) + el_B[E_x(\zeta_1 + \eta_2) + E_y(\eta_1 + \zeta_2)]. \tag{11}$$

The explicit form of the solutions for $\eta_i(t)$ and $\xi_i(t)$ are given in Appendix A.

Let us now now consider the complete Hamiltonian, including the contribution from the $\tilde{V}(\boldsymbol{r})$ potential. When the transformation induced by $W(t)$ is applied the Schrödinger equation in Eq. (1) becomes

$$P_0 \Psi^{(W)} = H_0 \Psi^{(W)} + V_W(t)\Psi^{(W)}, \tag{12}$$

where $\Psi^{(W)} = W(t)\Psi$ and

$$V_W(t) = W(t)\tilde{V}(\boldsymbol{r})W^{-1}(t) = W(t)V(\boldsymbol{r})W^{-1}(t) - V(\boldsymbol{r}). \tag{13}$$

Notice that the impurity potential acquires a time dependence brought by the $W(t)$ transformation. The problem is now solved in the interaction representation using first order time-dependent perturbation theory. In the interaction representation $\Psi_I^{(W)} = \exp\{iH_0 t\}\Psi^{(W)}$, and the Schrödinger equation becomes

$$i\partial_t \Psi_I^{(W)} = \{V_W(t)\}_I \Psi_I^{(W)}. \tag{14}$$

The equation is solved in terms of the evolution operator $U(t)$, in such a way that $\Psi_I^{(W)}(t) = U(t-t_0)\Psi_I^{(W)}(t_0)$. The solution of the evolution operator in first order perturbation theory is given by the expression

$$U(t) = 1 - i\int_{-\infty}^{t} dt' [W^\dagger(t')\tilde{V}(\boldsymbol{r})W(t')]_I, \tag{15}$$

which is explicitly evaluated in Appendix B. The interaction is adiabatically turned off as $t_0 \to -\infty$, in which case the asymptotic state is selected as one of the Landau-Floquet eigenvalues of H_0, i.e., $|\Psi_I^{(W)}(t_0)\rangle \to |\mu,k\rangle$. The solution to the original Schrödinger equation in Eq. (1) has been achieved by means of three successive transformations, which expressions have been explicitly obtained,

$$|\Psi_{\mu,k}(t)\rangle = W^\dagger \exp\{-iH_0 t\} U(t-t_0)|\mu,k\rangle. \tag{16}$$

As discussed in Appendix A the index k labels the degeneracy of the Landau-Floquet states. Selecting the P representation the dependence of the wave function on k becomes very simple. See Eq. (A6). For simplicity in what follows the index k will not be shown. The expression of the Kubo formula that will be derived in Sec. III requires the knowledge of the matrix elements of the momentum operator $\boldsymbol{\Pi}$,

$$\langle \Psi_\mu | \boldsymbol{\Pi}_i | \Psi_\nu \rangle = \langle \mu | U^\dagger(t-t_0)[W\boldsymbol{\Pi}_i W^\dagger]_I U(t-t_0)|\nu\rangle. \tag{17}$$

Let us first consider the term inside the square brackets. Using the explicit form of the operators in Eqs. (4), (6), and (10), it yields

$$W\boldsymbol{\Pi}_i W^\dagger = \begin{cases} \sqrt{eB}(P_1 - \eta_1), & i = x \\ \sqrt{eB}(Q_1 - \xi_1), & i = y. \end{cases} \tag{18}$$

If we now utilize the result for the evolution operator U given in Appendix B, we can explicitly work out the matrix elements of the momentum operator,

$$\langle \Psi_\mu | \boldsymbol{\Pi}_i | \Psi_\nu \rangle = \frac{\sqrt{eB}}{\sqrt{2}}(a_j\sqrt{\mu}e^{i\omega_c t}\delta_{\mu,\nu+1} + b_j\sqrt{\nu}e^{-i\omega_c t}\delta_{\mu,\nu-1}) + \sqrt{eB}\sum_l e^{i(\mathcal{E}_{\mu\nu}+\omega l - i\eta t)}\Delta_{\mu\nu}^{(l)}(j). \tag{19}$$

Here the following definitions were introduced: $\mathcal{E}_{\mu\nu} = \mathcal{E}_\mu - \mathcal{E}_\nu$, $a_j = b_j = 1$ if $j = x$, and $a_j = -b_j = -i$ if $j = y$, and $\Delta_{\mu\nu}^{(l)}(j)$ is given by

$$\Delta_{\mu\nu}^{(l)}(j) = \delta_{\mu\nu}[\rho_j\delta_{l,1} + \rho_j^*\delta_{l,-1}] - \frac{1}{\sqrt{2}}\left[\frac{a_j\tilde{q}^* C_{\mu\nu}^{(l)}}{\mathcal{E}_{\mu\nu} - \omega_c + \omega l - i\eta} + \frac{b_j\tilde{q}C_{\mu\nu}^{(l)}}{\mathcal{E}_{\mu\nu} + \omega_c + \omega l - i\eta}\right], \tag{20}$$

where $\tilde{q} = il_B(q_x - iq_y)/\sqrt{2}$, and the expressions for the functions ρ_i, and $C_{\mu,\nu}^{l}$ are worked out as

$$\rho_1 = \frac{el_B E_0(-i\omega\epsilon_x + \omega_c\epsilon_y)}{\omega^2 - \omega_c^2 + i\omega\Gamma_{rad}}, \quad \rho_2 = \frac{el_B E_0(\omega_c\epsilon_x + i\omega\epsilon_y)}{\omega^2 - \omega_c^2 + i\omega\Gamma_{rad}}, \tag{21}$$

and

$$C_{\mu,\nu}^{(l)} = \sum_i \int \frac{d^2q}{(2\pi)^2} V(\boldsymbol{q}) e^{-i\boldsymbol{q}\cdot\boldsymbol{r}_i} D_{\mu\nu}(q)\left(\frac{\Delta}{i|\Delta|}\right)^l \tilde{J}_l(|\Delta|), \tag{22}$$

where $\tilde{J}_l = J_l - \delta_{l,0}$, J_l being the Legendre polynomials, and $D_{\mu\nu}(q)$ is given in terms of the generalized Laguerre polynomials in Eq. (B4), and

$$\Delta = \frac{\omega_c l_B^2 eE_0}{\omega(\omega^2 - \omega_c^2 + i\omega\Gamma_{rad})}[\omega(q_x\epsilon_x + q_y\epsilon_y) + i\omega_c(q_x\epsilon_y - q_y\epsilon_x)]. \tag{23}$$

It is important to notice that the subtracted term $\tilde{J}_l = J_l - \delta_{l,0}$, has its origin in the fact that the impurity potential Eq. (2) includes only the dynamical effects, with the corresponding zero field term conveniently subtracted. This procedure is justified because the broadening effects produced by $V(\boldsymbol{r})$ are separately included via the Kubo formula. See Appendix E. The subtraction $\tilde{J}_l = J_l - \delta_{l,0}$ becomes essential, otherwise the longitudinal resistance would be dominated by the $l = 0$ term, producing incorrect results.

III. KUBO FORMULA FOR FLOQUET STATES

In this section we shall develop the Kubo formula that applies when the dynamics include Landau-Floquet states such as those in Eq. (16). We take the perturbing electric field to have the form $\boldsymbol{E}_{ext} = \boldsymbol{E}_{dc}\cos(\Omega t)\exp(-\eta|t|)$. The static limit is obtained with $\Omega \to 0$, and η represents the rate at which the perturbation is turned on and off. The perturbing electric field is included in the vector potential. As we are interested in the linear response the perturbing potential has the form

$$V_{ext} = \frac{1}{m}\boldsymbol{\Pi}\cdot\boldsymbol{A}_{ext}, \quad \boldsymbol{A}_{ext} = \frac{\boldsymbol{E}_{dc}}{\omega}\sin(\Omega t)\exp(-\eta|t|). \tag{24}$$

Besides the original Hamiltonian in Eq. (1), the complete Hamiltonian should include V_{ext} and the part of the disorder potential $[\Delta V(\boldsymbol{r}) = W^\dagger V(\boldsymbol{r})W]$ that was previously subtracted. [See Eq. (2).] Hence the total Hamiltonian H_T is written as

$$H_T = H + V_{ext} + \Delta V(\boldsymbol{r}). \tag{25}$$

The disorder potential $\Delta V(\boldsymbol{r})$ will induce broadening effects, and it will be included later. Then, the time evolution for the density matrix $\rho(t)$ obeys the von Neumann equation,

$$i\hbar\left(\frac{\partial\rho}{\partial t}\right) = [H + V_{ext}, \rho]. \tag{26}$$

Within the linear regime ρ is split in the sum $\rho = \rho_0 + \Delta\rho$. The zero order term ρ_0 must satisfy

$$i\hbar\left(\frac{\partial\rho_0}{\partial t}\right) = [H,\rho_0]. \tag{27}$$

The conditions required to solve this equation will be established below. The first order deviation $\Delta\rho$ then obeys

$$i\hbar\frac{\partial\Delta\rho}{\partial t} = [H,\Delta\rho] + [V_{ext},\rho_0]. \tag{28}$$

We shall now apply to this equation the three transformations that were utilized in the preceding section in order to solve the Schrödinger equation. Hence, in agreement with Eq. (16), $\widetilde{\Delta}\rho$ is defined as

$$\begin{aligned}\widetilde{\Delta}\rho(t) = {}& U_I^{\dagger}(t-t_0)\exp\{iH_0t\}W(t)\Delta\rho(t)W^{\dagger}(t)\\ &\times\exp\{-iH_0t\}U_I(t-t_0).\end{aligned} \tag{29}$$

In terms of the transformed density matrix $\widetilde{\Delta}\rho(t)$, Eq. (28) becomes

$$i\hbar\left(\frac{\partial\widetilde{\Delta}\rho}{\partial t}\right) = [\widetilde{V}_{ext},\widetilde{\rho}_0], \tag{30}$$

where $\widetilde{V}_{ext}$ and $\widetilde{\rho}_0$ are the external potential and quasiequilibrium density matrix transformed in the same manner as $\widetilde{\Delta}\rho$ is transformed in Eq. (29). The transformed quasiequilibrium density matrix is assumed to have the form $\widetilde{\rho}_0 = \Sigma_\mu|\mu\rangle f(\mathcal{E}_\mu)\langle\mu|$, where $f(\mathcal{E}_\mu)$ is the usual Fermi function and $\mathcal{E}_\mu$ the Landau-Floquet level. (See Appendix A). It is straightforward to verify that this selection guarantees that the quasiequilibrium condition in Eq. (27) is verified. The justification for selecting a Fermi-Dirac distribution in the quasienergy states is presented in Appendix C. It is shown that, under experimental conditions $(\tau_\omega \ll \tau_{tr} \ll \tau_{in})$, the elastic and inelastic relaxation processes can be neglected as compared to the external field effects. The solution of the Boltzmann equation yields, for a weak microwave intensity, a Fermi-Dirac distribution in the quasienergy states. The expectation value of Eq. (30) in the $|\mu\rangle$ base can now be easily calculated using Eqs. (16), (24), and (29). Solving the resulting equation with the initial condition, $\Delta\rho(t)\to 0$ as $t\to-\infty$, yields for $t<0$,

$$\begin{aligned}&\langle\mu|\widetilde{\Delta}\rho(t)|\nu\rangle\\ &\quad= \langle\Psi_\mu|\Delta\rho(t)|\Psi_\nu\rangle\\ &\quad= \frac{e\boldsymbol{E}_{dc}}{2}\int_{-\infty}^{t}\left[\frac{e^{i(\Omega-i\eta)t'}}{\Omega}f_{\mu\nu}\langle\Psi_\mu|\boldsymbol{\Pi}(t')|\Psi_\nu\rangle + (\Omega\to-\Omega)\right],\end{aligned} \tag{31}$$

where the definition $f_{\mu\nu}=f(\mathcal{E}_\mu)-f(\mathcal{E}_\nu)$ was used. Substituting the expectation value for the momentum operator given in Eq. (19), the integral in the previous equation is easily performed. The current density to first order in the external electric field can now be calculated from $\langle \boldsymbol{J}(t,\boldsymbol{r})\rangle = \mathrm{Tr}[\widetilde{\Delta}\rho(t)\widetilde{\boldsymbol{J}}(t)]$. The resulting expression represents the local density current. Here we are concerned with the macroscopic conductivity tensor that relates the spatially and time-averaged current density $\boldsymbol{j}=(\tau_\omega V)^{-1}\int_0^{\tau_\omega}dt\int d^2x\langle\boldsymbol{J}(t,\boldsymbol{r})\rangle$ to the averaged electric field, here $\tau_\omega=2\pi/\omega$. The macroscopic conductivity can now be worked out. Results for the dark and microwave-induced conductivities are quoted,

$$\begin{aligned}\boldsymbol{\sigma}_{xi}^{D} = \frac{e^2\omega_c^2}{i4\hbar}\sum_{\mu\nu}\Bigg\{&\frac{f_{\mu\nu}}{\Omega}\left[\frac{a_i\mu\delta_{\mu,\nu+1}}{\mathcal{E}_{\mu\nu}+\Omega-i\eta}+\frac{b_i\nu\delta_{\mu,\nu-1}}{\mathcal{E}_{\mu\nu}+\Omega-i\eta}\right]\\ &+(\Omega\to-\Omega)\Bigg\},\end{aligned} \tag{32}$$

$$\boldsymbol{\sigma}_{xi}^{\omega} = \frac{e^2\omega_c^2}{i4\hbar}\sum_{\mu\nu}\left\{\frac{f_{\mu\nu}}{\Omega}\sum_{l}\frac{\Delta_{\mu\nu}^{(l)}(i)\Delta_{\nu\mu}^{(-l)}(x)}{\mathcal{E}_{\mu\nu}+\omega l+\Omega-i\eta}+(\Omega\to-\Omega)\right\}. \tag{33}$$

In these expressions the external electric field points along the x axis. Hence, setting $i=x$ or $i=y$ the longitudinal and Hall conductivities can be selected. The denominators on the right-hand side (RHS) of the previous equations can be related to the advanced and retarded Green's functions $G_\mu^{\pm}(\mathcal{E}) = 1/(\mathcal{E}-\mathcal{E}_\mu\pm i\eta)$. To make further progress, the real and absorptive parts of the Green's functions are separated, taking the limit $\eta\to 0$ and using $\lim_{\eta\to0}1/(\mathcal{E}-i\eta)=\mathrm{P}1/\mathcal{E}+i\pi\delta(\mathcal{E})$, where P indicates the principal-value integral. As usual the real and imaginary parts contribute to the Hall and longitudinal conductivities, respectively. In what follows, details of the calculations are presented for the longitudinal microwave-induced conductivity. The corresponding dark conductivity expressions as well as the Hall microwave-induced conductance are quoted in Appendix D. Implementing the previous considerations and inserting a δ function, the longitudinal microwave-induced conductivity takes the form

$$\begin{aligned}\boldsymbol{\sigma}_{xx}^{\omega} = -\frac{e^2\omega_c^2}{4\hbar}\sum_{\mu\nu}\sum_{l}&\int d\mathcal{E}\,\delta(\mathcal{E}-\mathcal{E}_\mu)|\Delta_{\mu\nu}^{(l)}(x)|^2\\ &\times\left\{\frac{f(\mathcal{E}+\omega l+\Omega)-f(\mathcal{E})}{\Omega}\mathrm{Im}\,G_\nu(\mathcal{E}+\omega l+\Omega)\right.\\ &\left.+(\Omega\to-\Omega)\right\},\end{aligned} \tag{34}$$

where $\mathrm{Im}\,G_\nu(\mathcal{E})=\left(\frac{1}{2i}\right)[G_\nu^{+}(\mathcal{E})-G_\nu^{-}(\mathcal{E})]$. The static limit with respect to the external field is obtained, taking $\Omega\to0$. In the case of the impurity-assisted contribution an additional average over the impurity distribution has to be carried out. It is assumed that the impurities are not correlated, utilizing the explicit expressions for the velocity matrix elements in Eq. (20). The final result for the averaged microwave-induced longitudinal conductance is worked out as

$$\begin{aligned}\langle\boldsymbol{\sigma}_{xx}^{\omega}\rangle = \frac{e^2}{\pi\hbar}\int d\mathcal{E}&\sum_{\mu\nu}\sum_{l}\mathrm{Im}\,G_\mu(\mathcal{E})B^{(l)}(\mathcal{E},\mathcal{E}_\nu)\\ &\times\left\{\omega_c|\rho_1|^2\delta_{\mu\nu}(\delta_{l,1}+\delta_{l,-1})+n_{imp}l_B^2\right.\\ &\left.\times\int\frac{d^2q}{(2\pi)^2}q_y^2|\widetilde{J}_l(|\Delta|)V(\mathbf{q})D_{\mu\nu}(\widetilde{q})|^2\right\},\end{aligned} \tag{35}$$

where n_{imp} is the two-dimensional impurity density and the following function has been defined as

$$B^{(l)}(\mathcal{E},\mathcal{E}_\nu) = -\left[\frac{d}{d\mathcal{E}_0}\{[f(\mathcal{E}+l\omega+\mathcal{E}_0)-f(\mathcal{E})] \times \mathrm{Im}\, G_\nu(\mathcal{E}+l\omega+\mathcal{E}_0)\}\right]_{\mathcal{E}_0=0}. \quad (36)$$

The photoconductivity in Eq. (35) has a first contribution that depends on the ρ_1 factor (independent of the impurity concentration). It represents the direct cyclotron resonance heating arising when the $W(t)$ transformation is applied to the momentum operator. [See Eq. (18).] The impurity-induced contribution [second row in Eq. (35)] takes into account the dynamics produced by the magnetic and microwave fields combined with the resonant effect of the impurities; the information is contained in the complete wave function in Eq. (16).

The previous expression would present a singular behavior that is an artifact of the $\eta \to 0$ limit. This problem is solved by including the disorder broadening effects. A simple phenomenological prescription is dictated by simply retaining a finite value of η that is related to the quasiparticles' lifetime $(\eta = 2\pi/\tau_s)$.[27,28] According to this prescription the density of states (DOS) of the μ level would have a Lorentzian form,

$$\mathrm{Im}\, G_\mu(\mathcal{E}) = \frac{(\eta/2\pi)}{[(\mathcal{E}-\mathcal{E}_\mu)^2+\eta^2/4]}.$$

A more formal procedure requires us to calculate the broadening produced by the so far neglected part of the disorder potential $\Delta V(\boldsymbol{r})$. [See Eq. (25).] Fortunately, as explained in Appendix E, the calculation becomes equivalent to that carried out by Ando[30] and Gerhardts,[31] so the density of states for the μ Landau level can be represented by a Gaussian-type form,[32]

$$\mathrm{Im}\, G_\mu(\mathcal{E}) = \sqrt{\frac{\pi}{2\Gamma_\mu^2}}\exp[-(\mathcal{E}-\mathcal{E}_\mu)^2/(2\Gamma_\mu^2)],$$

$$\Gamma_\mu^2 = \frac{2\beta_\mu \hbar^2 \omega_c}{(\pi\tau_{tr})}. \quad (37)$$

The parameter β_μ in the level width takes into account the difference of the transport scattering time determining the mobility μ from the single-particle lifetime. In the case of short-range scatterers, $\tau_{tr}=\tau_s$ and $\beta_\mu = 1$. An expression for β_μ, suitable for numerical evaluation that applies for the long-range screened potential in Eq. (40) is given in Appendix E. β_μ decreases for higher Landau levels. This property becomes essential to generate NRS, because they only appear for a narrow Γ_μ, a condition that is satisfied around the Fermi level in the case of large filling factors.

Equations (35) and (36) contain the main ingredients that explain the huge increase observed in the longitudinal conductance (and resistance) when the material is irradiated by microwaves. In the standard expression for the Kubo formula there are no Floquet replica contributions, hence ω can be set to zero in Eq. (36). if that is the case $B^{(l)}$ becomes proportional to the energy derivative of the Fermi distribution that in the $T \to 0$ limit becomes of the form $\delta(\mathcal{E}-\mathcal{E}_F)$, and the conductivity is positive definite depending only on those states lying at the Fermi level. On the other hand, as a result of the periodic structure induced by the microwave radiation, $B^{(l)}$ contains a second contribution proportional to the derivative of the density of states, $(d/d\mathcal{E})\mathrm{Im}\, G_\nu(\mathcal{E}+l\omega)$. Due to the oscillatory structure of the density of states, this extra contribution takes both positive and negative values. According to Eq. (37) this second term (as compared to the first one) is proportional to the electron mobility. Hence, for sufficiently high mobility the new contribution dominates, leading to NRS. The former observation becomes fundamental, because in agreement with experiment our calculations show that NRS can only be induced in very high mobility samples. (See Fig. 1.)

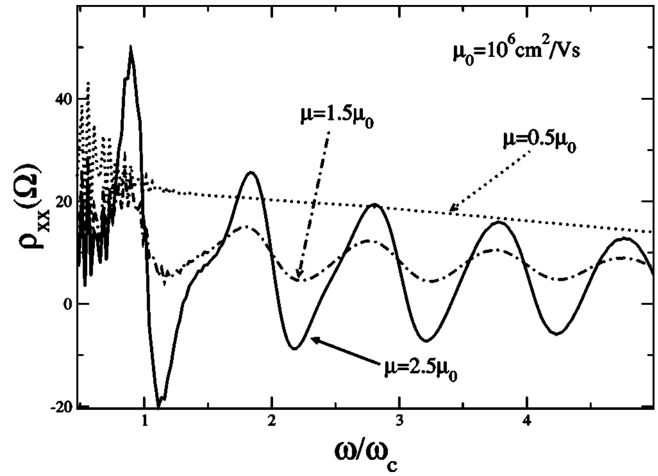

FIG. 1. Longitudinal resistivity as a function of $\epsilon=\omega/\omega_c$ for neutral impurity scattering and three values of the electron mobility, $\mu \approx 0.5\times10^6$ cm^2/V s (dotted line), $\mu \approx 1.5\times10^6$ cm^2/V s (dashed-dotted line), and $\mu \approx 2.5\times10^6$ cm^2/V s (continuous line). In the two former cases the oscillations follow a pattern with minima at $\epsilon = j+\delta$ and maxima at $\epsilon = j-\delta$, adjusted with $\delta \approx \frac{1}{5}$ NRS only appear when $\mu > \mu_{th} \sim 1.5\times10^6$ cm^6/V s. The values of the other parameters are the same as in Fig. 2.

As was mentioned in Sec. II the present method applies in general if $\tilde{V}(\boldsymbol{r})$ can be decomposed in its Fourier expansion [Eq. (3)], e.g., finite wavelength corrections, lattice periodic potential, impurity scattering, etc. The microwave radiation by itself only produces transitions between adjacent Landau levels [first term on the RHS of Eq. (35)], leading to the cyclotron peak. In the case of a periodic potential the resulting spectrum will be dominated by the region $q \approx 2\pi/a$, where a is the lattice parameter; for the experimental conditions $\lambda_B \gg a$ and the contribution is negligible. So we are led to analyze the impurity-assisted mechanism as a plausible scenario to explain the strong oscillatory structure of the magnetoresistance.

IV. RESULTS

The single-particle and transport relaxation rates induced by disorder are given by[29,33]

$$\left.\begin{array}{l}\dfrac{1}{\tau_s}\\ \dfrac{1}{\tau_{tr}}\end{array}\right\} = n_{imp}\frac{m^*}{\pi\hbar^3 k_F}\int_0^{2k_F} dq \frac{|V(q)|^2}{\sqrt{1-(q/2k_F)^2}} \times \left\{\begin{array}{l}1\\ \dfrac{q^2}{2k_F^2}\end{array}\right. , \tag{38}$$

where $V(q)$ is the Fourier transform of the impurity potential [Eq. (3)]. Remarkably, we have a consistent formalism in which (i) the photoconductivity [Eq. (35)], (ii) the relaxation rates [Eq. (38)], and (iii) the level broadening [Eqs. (37) and (E2)] can all be consistently calculated once $V(q)$ has been specified.

For neutral impurities the potential can be represented by a short range delta interaction. The coefficient in Eq. (3) corresponds to a constant that can be selected as $V(q) = 2\pi\hbar^2\alpha/m^*$. The expression in Eq. (38) is readily calculated to yield the same value for the single-particle and transport relaxation rates,

$$\frac{1}{\tau_{tr}^{(N)}} = \frac{1}{\tau_s^{(N)}} = \frac{4\pi^2\hbar}{m^*}\alpha^2 n_{imp}^{(N)}. \tag{39}$$

The upper index N labels the neutral impurity case. The evaluation of the photoconductivity [Eq. (35)] requires in general a time-consuming numerical integration. However, for moderate values of the microwave radiation the transitions are dominated by single photon exchange. In the neutral impurity case a very precise analytical approximation can be explicitly worked out. See Appendix F.

For charged impurities the Coulomb potential is long-range modified by the screening effects. Although electron motion is restricted to two dimensions, the electric field is three dimensional and there are contributions from the impurities localized within the doped layer of thickness d. The screened potential can then be represented in momentum coordinates by the expressions[29]

$$V(\vec{q}) = \frac{\pi\hbar^2}{m^*}\frac{e^{-qd}}{1+\dfrac{q}{q_{TF}}}, \quad q_{TF} = \frac{e^2 m^*}{2\pi\epsilon_0\epsilon_b\hbar^2}, \tag{40}$$

where the Thomas-Fermi (TF) approximation is implemented in order to calculate the di-electric function. Here ϵ_b represents the relative permittivity of the surrounding media. The expression in Eq. (40) corresponds to a screened potential, that in real space has a r^{-3} decay for large r. The rates in Eq. (38) can be evaluated numerically; however, an accurate analytical result is obtained by observing that the decaying exponential in Eq. (40) causes the integral to die off for $q \gg 1/|d|$ and the upper limit in the integral can therefore be set to infinity. Additionally for the relevant parameters (see below) the following conditions are observed $k_F \gg 1/|d|$ and $q_{TF} \gg 1/|d|$; consequently, it is reasonable to drop the factor q/q_{TF} in the denominator of Eq. (40) and replace the square root in the denominator of Eq. (38) by unity. These simplifications yield for the transport relaxation rate,

$$\frac{1}{\tau_{tr}^{(C)}} = \frac{\pi\hbar}{8m^*(k_F d)^3} n_{imp}^{(C)}. \tag{41}$$

The upper index C labels the charged impurity case. As expected, for charged remote impurities the single-particle lifetime differs from the transport lifetime. The approximated relation reads $\tau_{tr}^{(C)} \approx (2k_F d)^2 \tau_s^{(C)}$.[29]

The parameter values have been selected corresponding to reported experiments[2,3] in ultraclean $GaAs/Al_xGa_{1-x}As$ samples: effective electron mass $m^* = 0.067 m_e$, relative permittivity $\epsilon_b \approx 13.18$, Fermi energy $\mathcal{E}_F = 10$ meV, electron mobility $\mu \approx 0.1$–2.5×10^7 cm^2/V s, electron density $n = 3\times 10^{11}$ cm^{-2}, microwave frequencies $f = 50$–100 Ghz, magnetic fields in the range 0.05–0.4 T, and temperatures $T \approx 0.5$–2.5 K. The reported specimen is 5×5 mm^2 s. Typical microwave power is 10–40 mW; however, it is estimated[1] that the microwave power that impinges on the sample surface is of the order of 100–200 µW. Hence, the microwave electric field intensity is estimated as $|\vec{E}| \approx 1-3$ V/cm. Using these values, it is verified that the weak-overlapping condition holds: $\omega_c\tau_{tr} \sim 100$–$1000$.

Recalling that $\mu = e\tau_{tr}/m^*$, one can use Eqs. (39) and (41) to determine the values of n_{imp} corresponding to neutral or charged scatterers, respectively. For example, assuming $\mu \approx 2.5\times 10^6$ cm^2/V s, one estimates for neutral scattering $\alpha^2 n_{imp}^{(N)} \approx 1\times 10^7$ cm^{-2}. Although α and $n_{imp}^{(N)}$ are not separately fixed, one notices that the condition for the weak disorder potential as compared to the Landau energy can be expressed as $V(q)/(l_B^2\hbar\omega_c) = 2\pi\alpha \ll 1$; e.g., if $\alpha \sim 0.01$, then $n_{imp}^{(N)} \sim 10^{11}$ cm^{-2}. For charged impurities and taking a value for the separation d between the impurity and the 2DES as $d \approx 20$ nm yields $n_{imp}^{(C)} \approx 1.5\times 10^{11}$ cm^{-2}. In this case the weak disorder condition takes the form $V(q)/(l_B^2\hbar\omega_c) \sim \pi\exp(-2\pi d/l_B) \ll 1$ that is satisfied. A final remark is related to the radiative electron decay Γ_{rad} that determines the direct electron response to the microwave excitation [see Eqs. (23) and (A4)]. Following Ref. 34 Γ_{rad} is related to the radiative decay width that is interpreted as coherent dipole re-radiation of electromagnetic waves by the oscillating two-dimensional (2D) electrons excited by microwaves. Hence, it is given by $\Gamma_{rad} = ne^2/(6\epsilon_0 m^* c)$. Using the values of n and m^* given above it yields $\Gamma_{rad} \approx 0.38$ meV.

Adding the dark and microwave-induced conductivities, the total longitudinal, $\sigma_{xx} = \sigma_{xx}^D + \langle\sigma_{xx}^w\rangle$, and Hall, $\sigma_{xy} = \sigma_{xy}^D + \langle\sigma_{xy}^w\rangle$, conductivities are obtained. It should be pointed out that the interference between the dark and microwave contributions exactly cancels. The corresponding resistivities are obtained from the expression $\rho_{xx} = \sigma_{xx}/(\sigma_{xx}^2 + \sigma_{xy}^2)$ and $\rho_{xy} = \sigma_{xy}/(\sigma_{xx}^2 + \sigma_{xy}^2)$. The relation $\sigma_{xy} \gg \sigma_{xx}$ holds in general. Hence, it follows that $\rho_{xx} \propto \sigma_{xx}$ and the longitudinal resistivity follows the same oscillation pattern as that of σ_{xx}. The plots of the total longitudinal and Hall resistivities as a function of the magnetic field intensity are displayed in Fig. 2. Whereas the Hall resistance presents the expected monotonous behavior, the longitudinal resistance shows a strong oscillatory behavior with distinctive NRS. The behavior of the complete ρ_{xx} is contrasted with the dark contributions that present only the expected Shubnikov–de Hass oscillations.

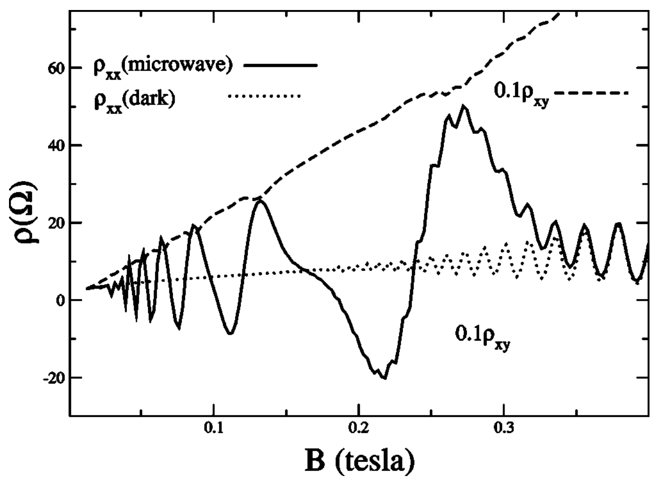

FIG. 2. Longitudinal resistance, both total (continuous line) and dark (dotted line) as a function of the magnetic field. The figure also includes the Hall resistance (dashed line, ρ_{xy} is rescaled by a factor $\frac{1}{10}$). Results corresponds to neutral impurity scattering obtained with the approximated solution (Appendix F) and the selected parameters are $\mu \approx 0.25\times 10^7$ cm^2/V s, $T\approx 1$ K, $f=100$ Ghz, $|\vec{E}| \approx 2.5$ V/cm, $\alpha^2 n_{imp}^{(N)} = 5\times 10^6$ cm^{-2}. The values of the other parameters used in the calculations are discussed in the text.

Figure 3 shows a comparison of the longitudinal resistivity as a function of ω/ω_c obtained for the case of neutral impurity scattering using both the approximated expression in Appendix F as well as the result of the numerical integration [Eq. (35)]. The electron mobility is selected as $\mu = 0.25\times 10^7$ cm^2/V s. The approximated analytical result shows a good agreement with the one obtained from the numerical integration. It should be remarked that the approximated expression includes only one-photon exchange processes, while the numerical result includes the possibility of multi-photon exchange. Hence, it is concluded that for the selected electric field intensity ($|\vec{E}| \sim 2.5$ V/cm), the one-photon processes dominate. Results are also presented for the case of charged impurity scattering but for $\mu = 2.5 \times 10^7$ cm^2/V s. In spite of the very different nature of the two physical processes and that the mobility is increased by an order of magnitude in the charged case, it is observed that the results for the neutral and charged cases are very similar. The similarity of both results is based on the following: (i) The increase in the mobility is compensated by the factor β_μ in Eq. (37), giving a similar broadening value. (ii) For the neutral case, $V(q)$ is constant over all the q-range of integration. Whereas for the charged case $V(q)$ varies according to the expression in Eq. (40). However, in both cases the integral in Eq. (35) is dominated by the region in which $q \approx 2\pi/l_B$.

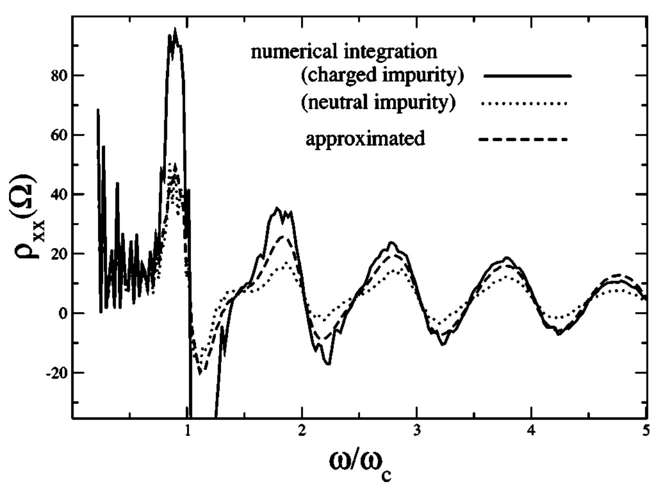

FIG. 3. Longitudinal resistance as a function of $\epsilon=\omega/\omega_c$ for neutral and charged impurities. Results for neutral impurities are obtained from the numerical integration (dotted line) and also using the analytical approximation discussed in Appendix F (dashed line) with the parameters $\mu\approx 0.25\times 10^7$ cm^2/V s, $\alpha^2 n_{imp}^{(N)} = 5 \times 10^6$ cm^{-2}. The continuous line corresponds to the charged impurity case with parameters $\mu \approx 2.5\times 10^7$ cm^2/V s, $n_{imp}^{(C)} = 1.5 \times 10^{11}$ cm^{-2}. The other parameters are the same as in Fig. 2.

One of the puzzling properties of the observed huge magnetoresistance oscillations is related to the fact that they appear only in samples with an electron mobility exceeding a threshold value μ_{th}. The phenomenon is absent in samples in which μ is slightly reduced. This behavior is well reproduced by the present formalism. Figure 1 displays the ρ_{xx} vs $\epsilon=\omega/\omega_c$ plot for neutral impurity scattering and three selected values of μ. For $\mu \approx 0.5\times 10^6$ cm^2/V s the previously known, almost linear behavior $\rho_{xx} \propto B$ is clearly depicted. As the electron mobility increases to $\mu \approx 1.5 \times 10^6$ cm^2/V s, the magnetoresistance oscillations are clearly observed; however, NRS only appear when the mobility is increased to $\mu \approx 2.5 \times 10^6$ cm^2/V s. It is observed that ρ_{xx} vanishes at $\epsilon = j$ for j integer. The period and phase of the oscillations follow a pattern very similar to the one observed in experiments,[2,4] with minima at $\epsilon = j+\delta$ and maxima at $\epsilon=j-\delta$, adjusted with $\delta \approx \frac{1}{5}$. It should be pointed out that this value of δ depends on the correct representation of the density of states. Using a Lorentzian form instead of the Gaussian in Eq. (37) would give $\delta \sim 1/10^{26}$. Similar behavior is observed for the charged impurity scattering case, but with the mobility threshold increased approximately by an order of magnitude $\mu_{th} \approx 2.5 \times 10^7$ cm^2/V s. The precise determination of μ_{th} depends of course on the selected values of the other parameters, mainly on the frequency and microwave intensity.

The early reported experiments[1–4] were carried out for a microwave radiation with transverse polarization with respect to the longitudinal current flow direction. It is clear, however, that the presence of the magnetic field induces a chirality in the system. The model can be used to test these effects. Figure 4 shows the results for different $\boldsymbol{E}$-field polarizations with respect to the current. In Fig. 4(a) it is observed that the amplitudes of the resistivity oscillation are slightly bigger for transverse polarization as compared to longitudinal polarization. This result is in agreement with the recent experiment,[4] in which it is reported that the selection of longitudinal or transverse polarization produces small differences. However, we propose that the more significant signatures will be only observable for circular polarization. Selecting negative circular polarization [see Fig. 4(b)], the oscillation amplitudes get the maximum possible value. Instead, for positive circular polarization an important reduc-

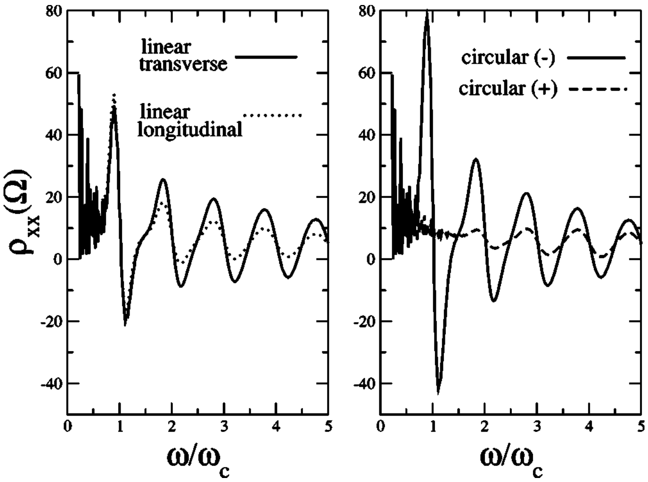

FIG. 4. Longitudinal resistance ρ_{xx} for neutral impurity scattering and various microwave E-field polarizations with respect to the current. In (a) the continuous and dotted lines correspond to linear transverse and longitudinal polarizations, respectively. (b) shows results for circular polarizations, left-hand (continuous line) and right-hand (dashed line). The values of the parameters are the same as in Fig. 2.

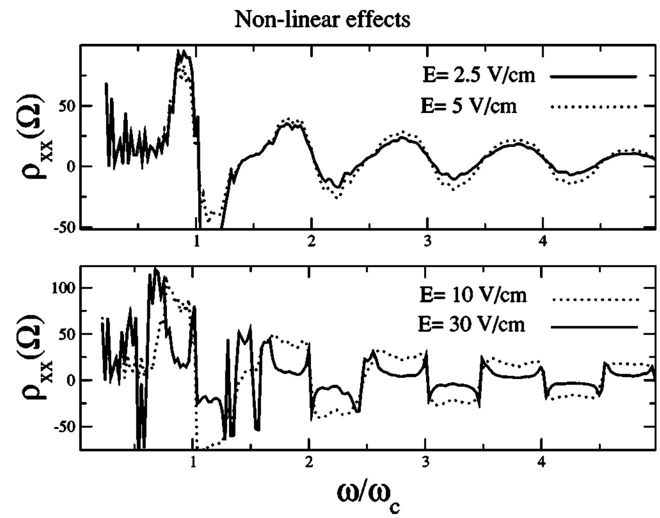

FIG. 5. Nonlinear effects in the longitudinal resistance ρ_{xx} for charged impurity scattering. (a) includes the ρ_{xx} vs $\epsilon=\omega/\omega_c$ plots for electric field intensities of $|\vec{E}|=2.5$ V/cm (continuous line) and $|\vec{E}|=5$ V/cm (dotted line). (b) displays results for $|\vec{E}|=10$ V/cm (dotted line) and $|\vec{E}|=30$ V/cm (continuous line). The parameter values are $\mu\approx 2.5\times 10^7$ cm^2/V s, $T\approx 1$ K, $f=100$ Ghz, and $n_{imp}^{(C)}=1.5\times 10^{11}$ cm^{-2}.

tion of the amplitude is observed leading to the total disappearance of the NRS. These results are understood, recalling that for negative circular polarization and $\omega\approx\omega_c$ the electric field rotates in phase with respect to the electron cyclotron rotation. Based on the present results, it will be highly recommended to carry out experiments for circular polarization configurations.

The present formalism can also be used in order to explore the nonlinear regime in which multiphoton exchange plays an essential role. As the microwave radiation intensity is increased, the analytical approximation breaks down and the numerical expression in Eq. (35) with higher multipole (l) terms needs to be evaluated. In the explored regime convergent results are obtained, including terms up to the $l=3$ multipole. Figure 5(a) displays ρ_{xx} vs ϵ plots for electric field intensities $|\vec{E}|=2.5$ V/cm and $|\vec{E}|=5$ V/cm, respectively. The increase on the field intensity produces a corresponding increase in the minima and maxima of ρ_{xx}, but apart from this, the qualitative behavior in both cases is similar. A further increase of the electric field intensity to $|\vec{E}|=10$ V/cm and $|\vec{E}|=30$ V/cm [Fig. 5(b)], takes us to the nonlinear regime in which a qualitatively new behavior is observed. For $\epsilon>2$ the same NRS are observed; however, the widths of these regions increase to include practically all the range from $\epsilon=j$ to $\epsilon=j+\frac{1}{2}$. Notice that the negative resistance minima does not have a monotonous dependence on $|\boldsymbol{E}|$. In fact for the strongest field intensity the minima approaches zero. Remarkably, for $|\vec{E}|=30$ V/cm and $\epsilon<2$, new negative resistance states associated with transitions by two microwave photons are observed near $\epsilon=\frac{1}{2}$ and $\epsilon=\frac{3}{2}$. The minima of these states are centered at $\epsilon_{\min}=0.52$ and $\epsilon_{\min}=1.52$, respectively. Evidence of ZRS associated with multiphoton processes has been already observed by Zudov *et al.*;[1] they reported structures with maxima near $\epsilon=\frac{1}{2}$ and $\epsilon=\frac{3}{2}$ and the corresponding minima centered around $\epsilon_{\min}=0.67$ and $\epsilon_{\min}=1.68$, respectively. Dorozhkin[5] and Willett *et al.*[6] have also reported ρ_{xx} minimum associated with $\epsilon=\frac{1}{2}$. Although the exact position of the minima and maxima of ρ_{xx} observed in Fig. 5(b) is not localized at the same position reported by Zudov *et al.*,[1] the general pattern is very similar, supporting the interpretation as multiphoton processes. Clearly, a more systematic analysis and further experimental studies are necessary.

Comparison with some other theoretical work is obliged. Previous work in Refs. 10–12 and 17 analyzed the effects of the microwave radiation on the electron scattering by impurities in the presence of a magnetic field. Durst *et al.*[12] consider an out-of-equilibrium calculation; Instead here a quasiadiabatic approximation is implemented, assuming that the system is thermalized in those states characterized by the Landau-Floquet spectrum. The similarity between some results in the present work and those of Durst *et al.*,[12] suggest that departure from equilibrium is not significant for the studied phenomenon. The present formalism extends and explores the impurity-assisted photoconductivity mechanism in detail. In this model the same disorder potential determines the broadening of the Landau levels, as well as the wave function that is used to evaluate the velocity matrix element. These matrix elements are incorporated into a Kubo-like formula that takes into account the Floquet structure of the system. As previously mentioned, there are alternative models in which the leading contribution arises from the modification of the electron distribution function induced by the microwave radiation. According to Dorozhkin[5] the negative resistance phenomena have their origin in a local population inversion that produces a change of sign of the $(\partial f/\partial\mathcal{E})$ term that appears in the conductivity. Although possible, the inversion of population requires rather strong microwave powers which were not achieved in the experiments.[34] Indeed, the inversion population is expected to be produced when the microwave energy exceeds the Fermi energy $(eE)^2/(m^*\omega^2) > E_F$. (See Appendix C) Clearly the estimated value for the threshold electric field $E_{th} \sim 1000$ V/cm highly exceeds the experimental microwave fields $E \sim 1-5$ V/cm. An interesting alternative explanation based on the modifications that the microwave radiation produces in the distribution function was recently presented by Dmitriev *et al.*[18] and Kennett *et al.*[20] In these publications it is assumed that the inelastic-scattering processes give the dominant contribution to the collision term of the kinetic equation. As explained in Appendix C however, under experimental conditions $\tau_\omega \ll \tau_{tr} \ll \tau_{in}$, and certainly the inelastic processes can be safely ignored as compared to the elastic processes. In fact we have presented an argument for a first approximation in which the distribution function is determined only by the microwave effects. It may be interesting for a future work to add to the present formalism the effects that elastic processes produce to the distribution function. In any case, we consider that the present results taken together with those of Refs. 10–12 and 17 consolidate the explanation of the photoconductivity oscillations and negative resistance states in terms of the microwave-disorder mechanism.

V. CONCLUSIONS

We have considered a model to describe the photoconductivity of a 2DES subjected to a magnetic field. We presented a thorough discussion of the method that allowed us to take into account the Landau and microwave contributions in a nonperturbative exact way while the impurity scattering effects are treated perturbatively. The method exploits the symmetries of the problem; the exact solution of the Landau-microwave dynamics [Eq. (9)] was obtained in terms of the electric-magnetic generators [Eq. (6)] as well the solutions to the classical equations of motion [Eq. (11)]. The spectrum and Floquet modes were explicitly worked out. In our model, the Landau-Floquet states act coherently with respect to the oscillating field of the impurities, that in turn induces transitions between these levels. Based on this formalism, a Kubo-like formula is provided. It takes into account the oscillatory Floquet structure of the problem. It should be stressed that the disorder potential is conveniently split [see Eqs. (2) and (25)] in such a way that it contributes both to the matrix elements of the velocity operator, as well as to the broadening of the Landau levels. Hence, we have a consistent formalism in which (i) the photoconductivity [Eq. (35)], (ii) the relaxation rates [Eq. (38)], and (iii) the level broadening [Eqs. (37) and (E2)] can all be consistently calculated once the disorder potential has been specified.

The expression for the longitudinal photoconductivity [Eq. (35)] contains the main ingredients that explain the huge increase observed in the experiments. As explained in Sec. III, the standard expression for the Kubo formula at low temperature is dominated by the states near to the Fermi level. On the other hand, as a result of the periodic structure induced by the microwave radiation the term $B^{(l)}$ contains a second contribution proportional to the derivative of the density of states, $(d/d\mathcal{E})\mathrm{Im}\, G_\nu(\mathcal{E}+l\omega)$. Due to the oscillatory structure of the density of states this extra contribution takes both positive and negative values. According to Eq. (37) this second term is proportional to the electron mobility. Hence for sufficiently high mobility the new contribution dominates leading to negative resistance states (NRS). This allows us to explain one of the puzzling properties of the observed huge magnetoresistance oscillations related to the fact that they appear only in samples with an electron mobility exceeding a threshold. This result is well reproduced by the present model. For the selected parameters, NRS emerge when the conditions $\mu \geqslant 2.5\times 10^6$ cm^2/V s (short-range disorder) and $\mu \geqslant 2.5\times 10^7$ cm^2/V s (long-range disorder) are satisfied. The oscillations follow a pattern with minima at $\epsilon = j+\delta$ and maxima at $\epsilon = j-\delta$, adjusted with $\delta \approx \frac{1}{5}$. These results are in reasonably good agreement with the observation of Mani *et al.*[2,4] They reported a similar pattern with $\delta \approx \frac{1}{4}$.

An interesting prediction of the present model is related to polarization effects that could be possibly observed in future experiments. While the results for the cases of linear transverse or longitudinal polarizations show small differences, the selection of circular polarized radiation leads to significant signatures. The maximum possible value for the oscillation amplitudes of ρ_{xx} appears for negative circular polarization. Instead, positive circular polarization yields an important reduction on the oscillation amplitudes and the total disappearance of the NRS. This result can be understood if one recalls that for negative circular polarization and $\omega \approx \omega_c$ the electric field rotates in phase with respect to the electron cyclotron rotation. The present results call for the importance of carrying out experiments with circular polarization configurations.

An analysis was presented in order to explore the nonlinear regime in which multiphoton exchange plays an essential role. The results suggest the existence of new NRS (which are expected to develop into ZRS) near $\epsilon = \frac{1}{2}$ and $\epsilon = \frac{3}{2}$. these states correspond to two-photon exchange processes and are in reasonable agreement with the reported experimental results.

Some final remarks are related to the limitations and possible extensions of the present work. In a first approximation we have not included the contribution of the elastic processes to the kinetic equation that determines the electron distribution. It will be interesting however, to extend the present calculations to include not only the dynamical effects produced by the impurity on the electron wave function, but also the modifications that they produce in the distribution function.

ACKNOWLEDGMENT

We acknowledge the partial financial support endowed by CONACyT through Grants No. 42026-F and No. 43110, and UNAM IN113305..

APPENDIX A: MICROWAVE-DRIVEN LANDAU PROBLEM

Equation (6) defines a canonical transformation from the variables $\{t,x,y;p_0,p_x,p_y\}$ to $\{Q_0,Q_1,Q_2;P_0,P_1,P_2\}$ in terms of the new variables. The Schrödinger equation (1) (without impurity potential) takes the form

$$P_0\Psi = \left\{\hbar\omega_c\left[\frac{(Q_1^2+P_1^2)}{2}\right] + el_BE_x(Q_1-P_2) + el_BE_y(Q_2-P_1)\right\}\Psi. \tag{A1}$$

The action of the transformation W defined in Eq. (10) over the (Q_μ, P_μ) variables can be easily calculated as

$$WQ_0W^\dagger = Q_0,$$

$$WP_0W^\dagger = P_0 + \dot{\eta}_1Q_1 + \dot{\zeta}_1P_1 + \dot{\eta}_2Q_2 + \dot{\zeta}_2P_2 - \dot{\zeta}_1\eta_1 - \dot{\zeta}_2\eta_2 + \mathcal{L},$$

$$WQ_1W^\dagger = Q_1 + \zeta_1, \quad WP_1W^\dagger = P_1 - \eta_1,$$

$$WQ_2W^\dagger = Q_2 + \zeta_2, \quad WP_2W^\dagger = P_2 - \eta_2. \tag{A2}$$

It can be verified that when the W transformation is applied to Eq. (A1), the second and third terms in the right-hand side exactly cancel with all the terms that appear in the expression for $WP_0W^\dagger$ (except P_0) if the functions η_i and ζ_i are selected to be solutions of the following differential equations:

$$\dot{\eta}_1 - \omega_c\zeta_1 = el_BE_x, \quad \dot{\zeta}_1 + \omega_c\eta_1 = -el_bE_y,$$

$$\dot{\eta}_2 = el_BE_y, \quad \dot{\zeta}_2 = -el_BE_x. \tag{A3}$$

But, these are exactly the classical equations of motion that follow when the variational principle is applied to the Lagrangian in Eq. (11). Hence, the W operator transforms the Schrödinger equation (A1) to the Landau eigenvalue problem with the Hamiltonian given in Eq. (9).

For the electric field consider the expression in Eq. (5). It is then straightforward to obtain the solutions to Eqs. (A3), adding a damping term that takes into account the radiative decay of the quasiparticle. The lines read

$$\eta_1 = el_BE_0\mathrm{Re}\left[\frac{-i\omega\epsilon_x + \omega_c\epsilon_y}{\omega^2-\omega_c^2+i\omega\Gamma_{rad}}e^{i\omega t}\right],$$

$$\eta_2 = el_BE_0\mathrm{Re}\left[\frac{\epsilon_y e^{i\omega t}}{i\omega}\right],$$

$$\zeta_1 = el_BE_0\mathrm{Re}\left[\frac{\omega_c\epsilon_x + i\omega\epsilon_y}{\omega^2-\omega_c^2+i\omega\Gamma_{rad}}e^{i\omega t}\right],$$

$$\zeta_2 = -el_BE_0\mathrm{Re}\left[\frac{\epsilon_x e^{i\omega t}}{i\omega}\right]. \tag{A4}$$

According to the Floquet theorem the wave function can be written as $\Psi(t)=\exp(-i\mathcal{E}_\mu t)\phi_\mu(t)$, where $\phi_\mu(t)$ is periodic in time, i.e., $\phi_\mu(t+\tau_\omega)=\phi_\mu(t)$. From Eq. (10) it is noticed that the transformed wave function $\Psi^W=W\Psi$ contains the phase factor $\exp(i\int^t\mathcal{L}dt')$. It then follows that the quasienergies and the Floquet modes can be deduced if we add and subtract to this exponential a term of the form $(t/\tau)\int_0^\tau\mathcal{L}dt'$. Hence, the quasienergies can be readily read off as

$$\mathcal{E}_\mu = \mathcal{E}_\mu^{(0)} + \mathcal{E}_{rad}, \quad \mathcal{E}_\mu^{(0)} = \hbar\omega_c\left(\frac{1}{2}+\mu\right),$$

$$\mathcal{E}_{rad} = \frac{e^2E_0^2[1+2\omega_c\mathrm{Re}(\epsilon_x^*\epsilon_y)/\omega]}{2m^*[(\omega-\omega_c)^2+\Gamma_{rad}^2]}. \tag{A5}$$

Here $\mathcal{E}_\mu^{(0)}$ are the usual Landau energies, and the induced Floquet energy shift is given by the microwave energy $\mathcal{E}_{rad}$. The corresponding time-periodic Floquet modes in the (P_1, P_2) representation are given by

$$\Psi_{\mu,k}(P) = \exp\{-i\sin(2\omega t)F(\omega)\}\phi_\mu(P_1)\delta(P_2-k). \tag{A6}$$

Here $\phi_\mu(P_1)$ is the harmonic oscillator function in the P_1 representation

$$\phi_\mu(P_1) = \langle P_1|\mu\rangle = \left(\frac{1}{\sqrt{\pi^{1/2}2^\mu\mu!}}\right)e^{-P_1^2/2}H_\mu(P_1), \tag{A7}$$

and $H_\mu(P_1)$ is the Hermite polynomial and the function $F(\omega)$ is given as

$$F(\omega) = \frac{\omega_c}{\omega}\left(\frac{eE_0l_B}{\omega^2-\omega_c^2}\right)^2\left[\omega^2-\omega_c^2+2\omega^2\epsilon_x^2-2\omega_c^2\epsilon_y^2 + \frac{\mathrm{Re}(\epsilon_x^*\epsilon_y)}{\omega\omega_c}(2\omega^4-\omega^2\omega_c^2+\omega_c^4)\right]. \tag{A8}$$

The wave function (A6) depends on the Landau (μ) and center guide (k) indexes; however, the spectrum (A6) is degenerate with respect to k. It is important to notice that $F(\omega)$ appear in the wave function phase that depends only on time. Hence its contribution to the expectation value of the momentum operator cancels exactly. Thus, contrary to what it is claimed in Ref. 15, the effect of the Floquet dynamics (without including an extra effect such as impurity scattering) cannot account for the explanation of the ZRS observed in recent experiments.

APPENDIX B: IMPURITY-INDUCED TRANSITIONS

In this appendix we consider the first order solution of the evolution operator $U(t)$ given by

$$U(t) = 1 - i\int_{-\infty}^t dt'[W^\dagger(t')\tilde{V}(\boldsymbol{r})W(t')]_I. \tag{B1}$$

The effect of the transformation induced by the W operator over the impurity potential can be easily evaluated considering the effect over the Fourier decomposition of $V(\boldsymbol{r})$ given in Eq. (3). Recalling that the x and y coordinates are written in terms of the new variables (Q_1, P_1, Q_2, P_2) by means of Eq. (7) and utilizing the transformation properties of the (Q_i, P_i) operators in Eq. (A2), it is readily obtained

$$W^\dagger(t)\exp\{i\boldsymbol{q}\cdot\boldsymbol{r}\}W(t) = \exp\{il_B(q_xP_2-q_yQ_2)\} \times\exp\{-il_B(q_xQ_1-q_yP_1)\} \times\exp\{il_B[q_x(\zeta_1+\eta_2)+q_y(\zeta_2+\eta_1)]\}. \tag{B2}$$

Using Eq. (A4) the third exponential in the previous equation can be recast in a compact form as $\exp\{-i\,\mathrm{Re}[\Delta\exp(i\omega t)]\}$, with Δ given in Eq. (23). This expression can be expanded as[35]

$$\exp\{-i\,\mathrm{Re}[\Delta\exp(i\omega t)]\} = \sum_{-l=\infty}^{l=\infty}\left(\frac{\Delta}{i|\Delta|}e^{i\omega t}\right)^{l} J_l(|\Delta|), \quad \text{(B3)}$$

with J_l the Legendre polynomials. For the second exponential notice that once that Q_1 and P_1 are replaced by the raising and lowering operators given in Eq. (8), one is lead to evaluate the matrix elements of the operator $D(\tilde{q})=\exp(\tilde{q}A_1^{\dagger}-\tilde{q}^*A_1)$ that generates coherent Landau states. A calculation yields

$$D^{\nu\mu}(\tilde{q}) = \langle\nu|D(\tilde{q})|\mu\rangle = e^{-\left(\frac{1}{2}\right)|\tilde{q}|^2}\begin{cases}(-\tilde{q}^*)^{\mu-\nu}\sqrt{\dfrac{\nu!}{\mu!}}L_{\nu}^{\mu-\nu}(|\tilde{q}|^2), & \mu>\nu \\ \tilde{q}^{\nu-\mu}\sqrt{\dfrac{\mu!}{\nu!}}L_{\mu}^{\nu-\mu}(|\tilde{q}|^2), & \mu<\nu,\end{cases} \quad \text{(B4)}$$

where L_{μ}^{μ} is the generalized Laguerre polynomial. With all these provisions the matrix element of the solution of the evolution operator in Eq. (B1) can be worked out as

$$\langle\mu|U(t)|\nu\rangle = \delta_{\mu\nu} - \sum_l\left[\frac{e^{i(\mathcal{E}_{\mu\nu}+\omega l)t}}{(\mathcal{E}_{\mu\nu}+\omega l - i\eta)}\right]C_{\mu\nu}^{(l)}. \quad \text{(B5)}$$

The explicit expression for $C_{\mu\nu}^{(l)}$ was given in Eq. (22).

APPENDIX C: MICROWAVE-DRIVEN DISTRIBUTION FUNCTION

Within the time relaxation approximation the Boltzmann equation can be written as

$$\frac{\partial f}{\partial t} + \frac{\partial f}{\partial \boldsymbol{p}}(e\boldsymbol{E} + e\boldsymbol{v}\times\boldsymbol{B}) = -\frac{f-f_F}{\tau_{tr}} - -\frac{f-f_F}{\tau_{in}},$$

where f_F is the Fermi-Dirac distribution and we distinguish between the elastic rate τ_{tr}^{-1} and inelastic or energy relaxation rate τ_{in}^{-1}. Under experimental conditions, $\tau_\omega \ll \tau_{tr} \ll \tau_{in}$, and certainly the inelastic processes can be safely ignored. Furthermore, due to the *ac*-electric field [Eq. (5)], the left-hand side of the previous equation is estimated to be of order f/τ_ω. Hence, in a first approximation the elastic scattering contribution can also be neglected. The resulting Vlasov equation has the exact solution $f(\boldsymbol{p},t)=f_F[\boldsymbol{p}-m^*\boldsymbol{v}(t)]$, where the velocity $\boldsymbol{v}(t)\equiv(\dot{\eta}_1,\dot{\zeta}_1)$ solves exactly the same classical equations of motion as given in Eq. (A3), and the initial condition is selected as $f\to f_F$ as the external electric field is switched off. In particular it is verified that $m^*|\boldsymbol{v}(t)|^2/2=\mathcal{E}_{rad}$ coincides with the Floquet energy shift produced by the microwave radiation [Eq. (A5)]. The steady-state distribution, evaluated at the Landau energy $\mathcal{E}=\mathcal{E}_{\mu}^{(0)}$, is obtained by averaging $f_F[\boldsymbol{p}-m^*\boldsymbol{v}(t)]$ over the oscillatory period

$$\langle f_F\rangle = \frac{1}{\tau_\omega}\int_0^{\tau_\omega} f_F\left(\mathcal{E}_{\mu}^{(0)} + \mathcal{E}_{rad} + 2\cos\omega_c t\sqrt{\mathcal{E}_{\mu}^{(0)}\mathcal{E}_{rad}}\right)dt.$$

For the experimental conditions it is verified that $\mathcal{E}_{rad}\ll\mathcal{E}_{\mu}^{(0)}$, thus expanding to first order one finds $\langle f_F\rangle \approx f_F(\mathcal{E}_{\mu}^{(0)}+\mathcal{E}_{rad}) = f_F(\mathcal{E}_\mu)$. Hence, it is verified that a rapid relaxation of the Fermi distribution to the quasienergy states is a reasonable assumption. The arguments presented in this appendix have been introduced by Mikhailov[34] in order to explore the possibility that the microwave radiation leads to a population inversion; however, it is concluded that it would require a rather high microwave intensity $\mathcal{E}_{rad}>\mathcal{E}_F$.

APPENDIX D: DARK AND HALL CONDUCTIVITIES

In Sec. III it was explained in detail the method to obtain the final expression for the microwave-induced magnetoresistance [Eq. (35)]. Working along a similar procedure the expression for the remaining conductivities are worked from Eqs. (32) and (33). First we quote the longitudinal dark conductance

$$\boldsymbol{\sigma}_{xx}^{D} = \frac{e^2\omega_c^2}{\pi\hbar}\sum_\mu \mu\int d\mathcal{E}\,\mathrm{Im}G_\mu(\mathcal{E})\frac{df}{d\mathcal{E}}\mathrm{Im}\,G_\mu(\mathcal{E}+\omega_c), \quad \text{(D1)}$$

whereas the dark Hall conductance is given by

$$\boldsymbol{\sigma}_{xy}^{D} = \frac{e^2\omega_c^2}{\pi\hbar}\sum_\mu \mu\int d\mathcal{E}\mathrm{Im}G_\mu(\mathcal{E}) \times[f(\mathcal{E}_\mu-\omega_c)-f(\mathcal{E})]\mathrm{P}\frac{1}{(\mathcal{E}-\mathcal{E}_\mu+\omega_c)^2}, \quad \text{(D2)}$$

where P indicates the principal-value integral. The impurity-assisted contributions require an additional average over the impurity distribution. It is assumed that the impurities are not correlated. The final result for the microwave-assisted longitudinal conductivity was quoted in Eq. (35). Following a similar procedure the microwave-assisted Hal conductivity is calculated to give

$$\langle\boldsymbol{\sigma}_{xy}^{\omega}\rangle = \frac{e^2\omega_c^2}{\pi\hbar}\int d\mathcal{E}\sum_{\mu\nu}\sum_l \mathrm{Im}\,G_\mu(\mathcal{E})[f(\mathcal{E}_\nu)-f(\mathcal{E}_\mu)] \times\left\{\delta_{\mu\nu}(\rho_1\rho_2^*\delta_{l,1}+\rho_1^*\rho_2\delta_{l,-1}) + n_{imp}\int d^2qT(\boldsymbol{q}) \times|\tilde{J}_l(|\Delta|)V(\boldsymbol{q})D_{\mu\nu}(\tilde{q})|^2\right\}, \quad \text{(D3)}$$

where the function $T(\boldsymbol{q})$ is defined as

$$T(\boldsymbol{q}) = \omega_c l_B^2\frac{q_x^2+q_y^2}{\mathcal{E}+\omega l-\mathcal{E}_\nu\,|(\mathcal{E}+\omega l-\mathcal{E}_\nu)^2-\omega_c^2|^2}. \quad \text{(D4)}$$

APPENDIX E: LANDAU DENSITY OF STATES

A detailed calculation of the density of states incorporating all the elements that contribute to the system under study is beyond the scope of the present paper; however, it can be argued that the expression given in Eq. (37) for the DOS is expected to be a reasonable selection under some consistent approximations. Let us consider the Green's function associated with the Hamiltonian $H+\Delta V$, where H is given in Eq. (1) and $\Delta V = W^{\dagger} V W$ is the subtracted part of the disorder potential [Eq. (25)]. As explained in Sec. III, the Kubo formula [Eqs. (32) and (33)] was deduced using the wave function obtained after the three transformations in Eq. (16) are applied to the Landau states. Hence, ΔV is transformed according to

$$\Delta\widetilde{V}(t) = U_I^{\dagger}(t-t_0)\exp\{iH_0 t\}W(t)\Delta V W^{\dagger}(t)\exp\{-iH_0 t\}U_I(t-t_0)$$

[see Eq. (29)]. Notice that (i) the W transformation cancels exactly, (ii) both ΔV and the first order correction to $U_I(t-t_0)$ are proportional to V, and hence, considering linear terms on V we can set $U_I(t-t_0)\approx 1$, and (iii) finally when evaluated in the $|\mu\rangle$ base and neglecting inter-Landau mixing, the contributions from $\exp\{-iH_0 t\}$ cancel out. Hence, $\Delta\widetilde{V}\approx V(\boldsymbol{r})$, and the problem under consideration reduces to evaluate the density of states produced by a magnetic field and a disorder potential $V(\boldsymbol{r})$ of the form given in Eq. (3); but this is precisely the problem considered some ago time by by Ando[30] and Gerhardts.[31] The density of states is well represented by the Gaussian expression in Eq. (37), and the level broadening neglecting couplings between different Landau levels is taken from Ref. 32,

$$\Gamma_{\mu}^2 = 8 * \pi l_B^2 n_{imp}\int \frac{d^2 r}{2\pi l_B^2}\int \frac{d^2 r'}{2\pi l_B^2} V(\boldsymbol{r})V(\boldsymbol{r}')[D^{\mu\mu}(|\boldsymbol{r}-\boldsymbol{r}'| \times(\sqrt{2}l_B))]^2, \tag{E1}$$

where $D^{\mu\mu}$ is given in Eq. (B4). For the delta short range scatterers the previous expression is readily evaluated, yielding the result in Eq. (37) with $\beta_{\mu}=1$. In the case of the charged impurity disorder, after the substitution of the Fourier decomposition [Eq. (3)] and using Eq. (40) it is verified that Γ_{μ} is again given by the expression in Eq. (37), but the factor β_{μ} is given by

$$\beta_{\mu} = 16\pi(k_F d)^3\int_0^{\infty} q\frac{\exp\left[-\sqrt{8}\frac{d}{l_B}q\right]}{\left(1+\frac{\sqrt{2}q}{l_B q_{TF}}\right)^2}[D^{\mu\mu}(q)]^2 dq. \tag{E2}$$

Previous analyse of the Landau level broadening were carried out, for example,[30] for a Gaussian potential $V(\boldsymbol{r}) \sim e^{r^2/d^2}$. However, as mentioned in Sec. IV the actual situation corresponds to a screened potential that in real space has a r^{-3} decay for large r. As mentioned in Sec. III the value of β_{μ} decreases for higher Landau levels. For example for the selected parameter, we have $\beta_0=108$, $\beta_{30}=14$, and $\beta_{50}=11$.

APPENDIX F: APPROXIMATED ONE-PHOTON EXCHANGE PHOTOCONDUCTIVITY

The microwave-induced longitudinal [Eq. (35)] conductivity requires the numerical evaluation of a time-consuming integral given by

$$S_l = \int d^2 q K(\boldsymbol{q})|J_l(|\Delta|)V(\boldsymbol{q})D_{\mu\nu}(\widetilde{q})|^2.$$

However, if we consider the regime of moderate microwave intensity and assume neutral impurity scattering, a very useful analytical approximation can be worked out. For neutral impurity scatterers, the potential is assumed to be of the short range delta form, hence the Fourier coefficient in Eq. (3) is given by $V(\boldsymbol{q})=2\pi\hbar^2\alpha/m^*$. The $D_{\mu\nu}(\widetilde{q})$ term contains an exponential factor that represents a cutoff for large q. Then according to Eq. (23) for moderate values of the microwave electric field the Δ term is small and the leading contributions arise from the $l=\pm 1$ factors that correspond to the single photon exchange contribution. Using the approximation $J_1(z)\approx z/2$ one is lead to evaluate

$$S_{\pm 1} = \frac{2\pi\hbar^2\alpha}{m^*}\int d^2 q K(\boldsymbol{q})|\Delta|^2 D_{\mu\nu}(\widetilde{q})^2. \tag{F1}$$

The angular integration is straightforward, while the integral over the $q=\sqrt{q_x^2+q_y^2}$ leads, after a change of variable $\xi=q^2$, to an integral of the form

$$\int_0^{\infty} d\xi e^{-\xi}\xi^{\mu-\nu+2}(L_{\nu}^{\mu-\nu})^2, \tag{F2}$$

which is explicitly evaluated with the help of the recurrence relation $xL_n^k=(2n+k+1)L_n^k-(n+k)L_{n-1}^k-(n+1)L_{n+1}^k$ and the integral[35]

$$\int_0^{\infty} d\xi e^{-\xi}\xi^k L_n^k L_m^k = \frac{(n+k)!}{n!}\delta_{mn}. \tag{F3}$$

The final result reads

$$S_{\pm 1} = \frac{\pi\hbar^2\alpha\omega^2|E|^2 I_{\mu\nu}}{8m^*\omega_c^2|\omega^2-\omega_c^2+i\omega\Gamma|^2}[\omega^2(1+2|\epsilon_y|^2) + \omega_c^2(1+2|\epsilon_x|^2) - 8\omega\omega_c \mathrm{Im}(\epsilon_x^*\epsilon_y)], \tag{F4}$$

where

$$I_{\mu\nu} = 6\left(\mu+\frac{1}{2}\right)\left(\mu+\frac{1}{2}\right)+(\mu-\nu)^2+\frac{1}{2}. \tag{F5}$$

These expressions greatly simplify the numerical calculations, and as discussed in Sec. IV they provide a very accurate approximation to the exact result.

*Email address: torres@fisica.unam.mx
†Email address: akb@correo.azc.uam.mx

[1] M. A. Zudov, R. R. Du, J. A. Simmons, and J. L. Reno Phys. Rev. B **64**, 201311(R) (2001).
[2] R. G. Mani, J. H. Smet, K. von Klitzing, V. Narayanamurti, W. B. Johnson, and V. Umansky, Nature (London) **420**, 646 (2002); Phys. Rev. Lett. **92**, 146801 (2004).
[3] M. A. Zudov, R. R. Du, L. N. Pfeiffer, and K. W. West, Phys. Rev. Lett. **90**, 046807 (2003).
[4] R. G. Mani, Physica E (Amsterdam) **22**, 1 (2004).
[5] S. I. Dorozhkin. JETP Lett. **77**, 577 (2003).
[6] R. L. Willett, L. N. Pfeiffer, and K. W. West, Phys. Rev. Lett. **93**, 026804 (2004).
[7] M. A. Zudov, Phys. Rev. B **69**, 041304(R) (2004).
[8] A. E. Kovalev, S. A. Zvyagin, C. R. Bowers, J. L. Reno, and J. A. Simmons, Solid State Commun. **1130**, 379 (2004).
[9] S. A. Studenikin, M. Potemski, A. Sachrajda, M. Hilke, L. N. Pfeiffer, and K. W. West, cond-mat/0404411 (unpublished).
[10] V. I. Ryzhii, Sov. Phys. Solid State **11**, 2078 (1970).
[11] V. I. Ryzhii and R. Suris, J. Phys.: Condens. Matter **15**, 6855 (2003).
[12] A. C. Durst, S. Sachdev, N. Read, and S. M. Girvin, Phys. Rev. Lett. **91**, 086803 (2003).
[13] A. V. Andreev, I. L. Aleiner, and A. J. Millis, Phys. Rev. Lett. **91**, 056803 (2003).
[14] P. W. Anderson and W. F. Brinkman, cond-mat/0302129. (unpublished).
[15] J. Shi and X. C. Xie, Phys. Rev. Lett. **91**, 086801 (2003).
[16] X. L. Lei and S. Y. Liu, Phys. Rev. Lett. **91**, 226805 (2003).
[17] M. G. Vavilov and I. L. Aleiner, Phys. Rev. B **69**, 035303 (2004).
[18] I. A. Dmitriev, A. D. Mirlin, and D. G. Polyakov Phys. Rev. Lett. **91**, 226802 (2003).
[19] I. A. Dmitriev, M. G. Vavilov, I. L. Aleiner, A. D. Mirlin, and D. G. Polyakov, cond-mat/0310668 (unpublished), cond-mat/0409590 (unpublished).
[20] M. P. Kennett, J. P. Robinson, N. R. Cooper, and V. Fal'ko, cond-mat/0410064 (unpublished).
[21] K. Husimi, Prog. Theor. Phys. **9**, 381 (1953).
[22] A. Kunold and M. Torres, Phys. Rev. B **61**, 9879 (2000).
[23] M. Torres and A. Kunold, Phys. Lett. A **323**, 2890 (2004).
[24] N. Ashby and S. C. Miller, Phys. Rev. **139**, A428 (1965).
[25] A. Kunold and M. Torres, Ann. Phys. **315**/2 532 (2005).
[26] M. Torres and A. Kunold, cond-mat/0409588 (unpublished).
[27] G. Mahan, *Many-Particle Physics*, 2nd ed. (Plenum Press, New York, 1993).
[28] J. Sinova, T. Jungwirth, J. Kucera, and A. H. MacDonald, Phys. Rev. B **67**, 235203 (2003).
[29] J. H. Davies, *The Physics of Low-Dimensional Semiconductors* (Cambridge University Press, Cambridge, 1998).
[30] T. Ando and Y. Uemura, J. Phys. Soc. Jpn. **36**, 959 (1974).
[31] R. R. Gerhardts, Z. Phys. B **21**, 275 (1975); **21**, 285 (1975).
[32] T. Ando, A. B. Fowler, and F. Stern, Rev. Mod. Phys. **54**, 437 (1982).
[33] T. Dittrich, P. Hanggi, G. L. Ingold, B. Kramer, G. Schon, and W. Zwerger, *Quantum Transport and Dissipation* (Wiley-VCH, New York, 1998).
[34] S. A. Mikhailov, cond-mat/0405136 (unpublished).
[35] *Handbook of Mathematical Functions*, edited by M. Abramowitz and I. A. Stegun (Dover Publications, New York, 1972).